Gene Therapy (2014), 1–7

www.nature.com/gt

SHORT COMMUNICATION

Adenoviral transfer of human *aquaporin-1* gene to rat liver improves bile flow in estrogen-induced cholestasis

J Marrone[1], GL Lehmann[2], LR Soria[1], JM Pellegrino[1], S Molinas[1] and RA Marinelli[1]

Estrogens can cause liver cholestatic disease. As downregulation of hepatocyte canalicular aquaporin-8 (AQP8) water channels has been involved in estrogen-induced bile secretory failure, we tested whether the archetypal water channel AQP1 improves 17α-ethinylestradiol (EE)-induced cholestasis. EE administration to rats reduced bile flow by 50%. A recombinant adenoviral (Ad) vector encoding human AQP1 (*h*AQP1), Ad*h*AQP1, or a control vector was administered by retrograde bile ductal infusion. Hepatocyte canalicular *h*AQP1 expression was confirmed by liver immunostaining and immunoblotting in purified membrane fractions. Accordingly, canalicular osmotic water permeability was markedly increased. Bile flow, either basal or bile salt-stimulated was significantly augmented by over 50%. The choleretic efficiency of endogenous bile salts (that is, volume of bile per μmol of excreted bile salt) was significantly increased by 45% without changes in the biliary bile salt composition. Our data suggest that the adenoviral transfer of *hAQP1* gene to the livers of EE-induced cholestatic rats improves bile flow by enhancing the AQP-mediated bile salt-induced canalicular water secretion. This novel finding might have potential therapeutic implications for cholestatic diseases.

Gene Therapy advance online publication, 11 September 2014; doi:10.1038/gt.2014.78

INTRODUCTION

Cholestasis is characterized by impairment of bile formation and it is caused by many liver diseases. Chronic cholestasis can progress toward biliary cirrhosis and liver failure requiring liver transplantation. Estrogens are well known to cause liver cholestatic disease, whose clinical manifestations are cholestasis associated with pregnancy or postmenopausal replacement therapy and oral contraceptive-induced cholestasis.[1] Experimental cholestasis induced by estrogen administration to rodents, mainly 17α-ethinylestradiol (EE), is an established experimental model used to investigate the mechanisms of estrogen-induced bile secretory dysfunction.[2] Aquaporins (AQPs) are a family of protein channels that facilitates the osmotically driven water movement across cell membranes.[3] AQP8, localized in the canalicular plasma membrane domain of hepatocytes, has been involved in water transport during bile formation.[4,5] Previously, we suggested that a reduced canalicular membrane water permeability resulting from downregulation of hepatocyte AQP8 expression contributes to the molecular pathogenesis of EE-induced cholestasis.[6] Adenovirus vectors are widely used for *in vivo* gene therapy. The gene transfer of the archetypal human water channel AQP1 via the adenoviral vector Ad*h*AQP1 has been successfully used to restore normal salivary flow to irradiated hypofunctional salivary gland of experimental animals[7,8] and humans.[9] The purpose of this study was to test whether the administration of the Ad*h*AQP1 vector can promote AQP1-mediated canalicular water secretion and improve bile secretory failure in rats with estrogen-induced cholestasis.

RESULTS AND DISCUSSION

The major finding in this study relates to the functional significance of canalicularly expressed *h*AQP1 water channels in the hepatocyte bile secretion in cholestasis. We provide experimental evidence that the adenoviral gene delivery of *h*AQP1 to livers of EE-induced cholestatic rats, (i) induced *h*AQP1 canalicular expression and consequently, increased the canalicular osmotic membrane water permeability; (ii) increased bile flow under basal and taurocholate-stimulated conditions; and (iii) enhanced the choleretic efficiency of endogenous bile salts. An important role for AQP-mediated canalicular water permeability in improving hepatocyte bile secretory dysfunction in estrogen-induced cholestasis is suggested.

Hepatocyte expression of *h*AQP1 in Ad*h*AQP1-transduced rats

Figure 1a shows immunohistochemistry and confocal immunofluorescence microscopy for AQP1. In agreement with the reported endogenous hepatic AQP1 expression,[10] AQP1 staining was intense in peribiliary vascular endothelia and weak in bile duct epithelial cells (cholangiocytes) of rat livers transduced with control vector, but absent in hepatocytes. Similar results were observed in livers from EE-treated rats transduced with control vector (not shown). Ad*h*AQP1 administration in non-cholestatic and EE-treated rats induced the expression of *h*AQP1 in hepatocytes (Figure 1a). Cholangiocytes did not show any clear increased staining for AQP1 (Figure 1a). In hepatocytes, *h*AQP1 was primarily located in plasma membranes without accumulation in intracellular organelles. Importantly, *h*AQP1 expression could be observed in the bile secretory pole of hepatocytes, that is, the canalicular plasma membrane (Figure 1a). The hepatocyte plasma membrane expression of *h*AQP1 did not differ between normal and EE-treated rats (Figure 1b), suggesting that EE-induced cholestasis did not impair vector infection and *h*AQP1 expression. Immunoblotting studies confirmed the expression of *h*AQP1

[1]Instituto de Fisiología Experimental, Consejo Nacional de Investigaciones Científicas y Técnicas (CONICET), Facultad de Ciencias Bioquímicas y Farmacéuticas, Universidad Nacional de Rosario, Rosario, Argentina and [2]Margaret Dyson Vision Research Institute, Weill Cornell Medical College, New York, NY, USA. Correspondence: Dr RA Marinelli, Instituto de Fisiología Experimental, Facultad de Ciencias Bioquímicas y Farmacéuticas, Universidad Nacional de Rosario, Suipacha 570, Rosario 2000, Argentina.
E-mail: rmarinel@unr.edu.ar or marinelli@ifise-conicet.gov.ar
Received 4 April 2014; revised 1 July 2014; accepted 9 July 2014

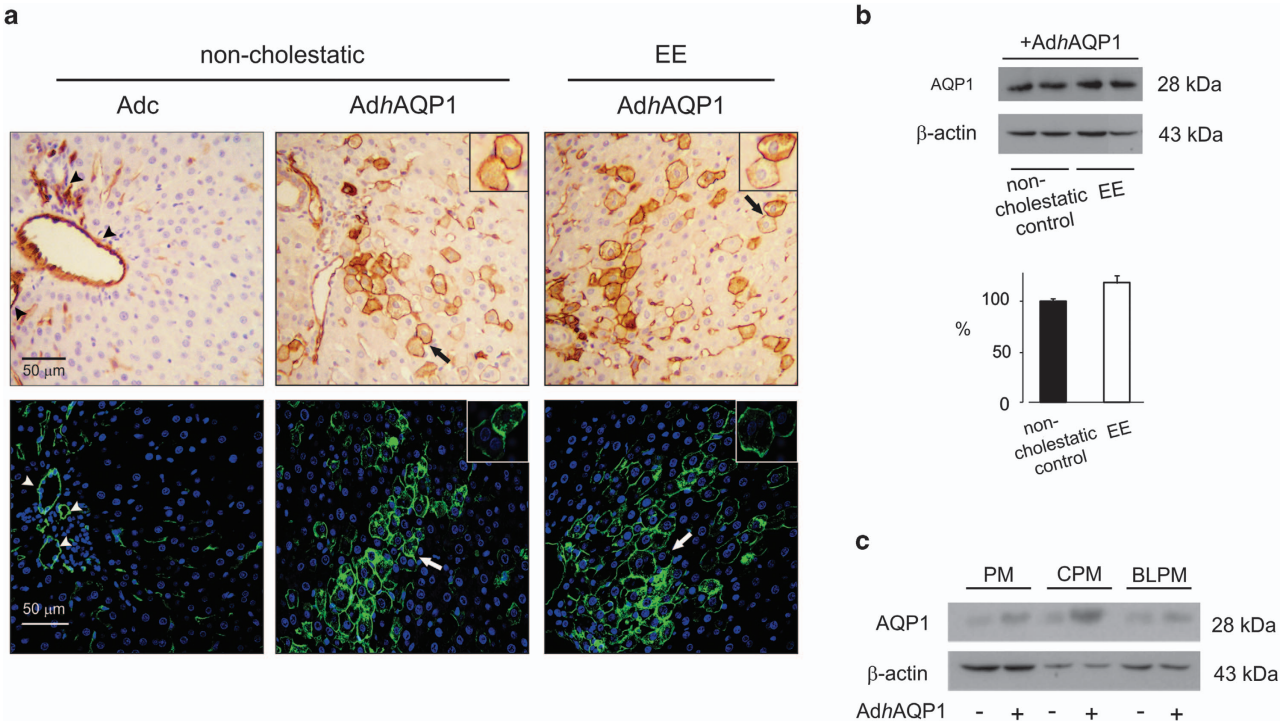

Figure 1. Hepatocyte expression of *h*AQP1 in normal and EE-cholestatic rats after Ad*h*AQP1 delivery. The induction of cholestasis by EE and the delivery of vectors were detailed in Materials and Methods. The experiments were performed 72 h after adenoviral infusion (that is, on the 6th day after starting EE treatment). (**a**) Top panel: immunohistochemistry for AQP1 in paraffin liver sections from Ad*h*AQP1-transduced normal and cholestatic rats. As expected,[10] non-cholestatic controls transduced with Adc showed endogenous AQP1 immunoreactivity (brown staining) only in peribiliary vascular endothelia (intense staining) and cholangiocytes (weak staining) (arrow heads). Immunoreactivity for AQP1 in Ad*h*AQP1-transduced rats was mostly observed on the canalicular and basolateral plasma membranes of hepatocytes (arrows, see inset). No staining was observed in experiments omitting AQP1 primary antibody (data not shown). Bottom panel: immunofluorescence localization of AQP1 viewed by laser scanning confocal microscopy. Results are in accordance with immunohistochemistry. (**b**) Anti-AQP1 immunoblot of hepatic plasma membranes from normal and cholestatic rats. Lanes were loaded with 25 μg of proteins. The blots were reprobed by using anti-β-actin antibody as a control for equal protein loading. Densitometric analysis of four separate experiments in each group. Data (means ± s.e.m.) are expressed as percentage of controls. (**c**) Anti-AQP1 immunoblot of hepatic canalicular (CPM) and basolateral (BLPM) plasma membrane fractions from cholestatic rats transduced with Ad*h*AQP1 or control vector. Lanes were loaded with 20 μg of proteins. The blots were reprobed by using anti-β-actin antibody as a control for equal protein loading. PM, total plasma membranes.

mainly in hepatocyte canalicular plasma membranes of EE-treated rats (Figure 1c).

To determine whether the expressed *h*AQP1 protein was functional, canalicular osmotic water permeability was measured by stopped-flow spectrophotometry. Canalicular membranes from cholestatic rats transduced with Ad*h*AQP1 vector showed fivefold average increase in water permeability over cholestatic rats transduced with control vector (Figure 2). This indicates that a functional *h*AQP1 protein was expressed in hepatocyte canaliculi of cholestatic rats.

Under our experimental conditions, Ad*h*AQP1 administration induced *h*AQP1 expression in roughly 20% of hepatocytes based on immunostainings (Figure 1a) and the percentage of canalicular vesicles with high water permeability (see Figure 2 and corresponding legend). This percentage of hepatocytes transduced via a retrograde adenovector infusion is in fairly good agreement with previous reports.[11,12] It is important to mention that periportal hepatocytes (the hepatocytes closest to the portal venules in the liver acinus) are predominantly transduced after adenoviral retrograde bile ductal infusion[12] and that these cells are the primary hepatocytes for bile formation.[13] Thus retrograde biliary infusion induced suitable *h*AQP1 hepatocyte expression, in addition to cause no significant adverse effects as shown in Table 1 and reported previously.[12] In accordance, Ad*h*AQP1 transfer via retrograde ductal infusion to salivary glands shows no significant hepatic toxicity.[14] Intrabiliary infusion allows the delivery of adenovirus to hepatocytes with minimal leak outside the liver because of the anatomical constraints of the biliary tract[15] and besides, excess adenovirus is delivered immediately into the duodenum and excreted in the stool. Thus repetitive transgene hepatic expression could be achieved by intrabiliary infusion without immunosuppression.[16]

Bile flow in Ad*h*AQP1-transduced cholestatic rats

Bile formation by hepatocytes is an osmotic secretory process resulting from the canalicular secretion of water in response to osmotic gradients created by the active transport of solutes, primarily bile salts and other organic anions. Thus bile flow is ultimately dependent on the canalicular expression of transporters such as the bile salt export pump Bsep/Abcb11 and the multidrug-resistant protein Mrp2/Abcc2, and the water permeability of the canalicular plasma membrane domain mainly determined by AQPs.[4,5,17] Impairment of these basic processes of canalicular fluid secretion is believed to be the primary event in the development of cholestasis induced by estrogen.[4,18,19]

Thus we studied whether the AQP1-induced increase in canalicular water permeability could affect the flow of bile in cholestatic rats. As shown in Figure 3a, bile flow was increased by 51% in cholestatic rats transduced with Ad*h*AQP1 vector. As bile salts are key solutes in bile formation by hepatocytes, we

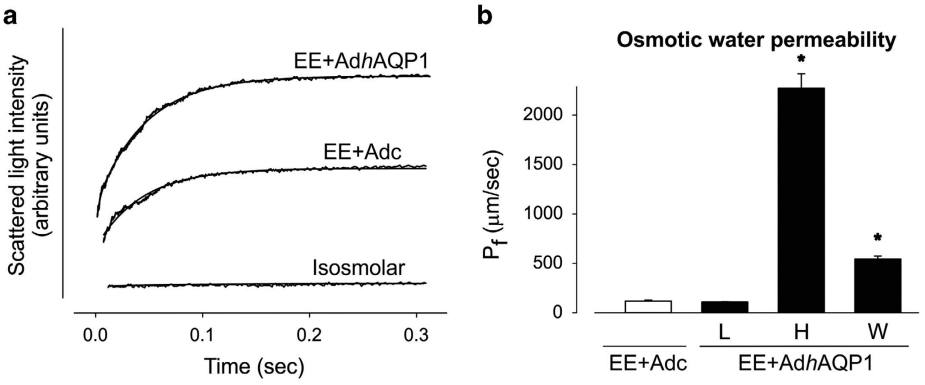

Figure 2. Water permeability of hepatic canalicular membranes from EE-cholestatic rats transduced with Ad*h*AQP1. The induction of cholestasis by EE and the delivery of vectors were detailed in Materials and Methods. The experiments were performed 72 h after adenoviral infusion (i.e., on the 6th day after starting EE treatment). The time course of scattered light intensity was measured for a 250 mosM hypertonic sucrose gradient by stopped flow spectrophotometry. (**a**) Typical tracings of a time course of scattered light intensity (osmotic water transport), along with a single exponential fit for canalicular vesicles from a cholestatic liver treated with control vector and a double-exponential fit for canalicular vesicles from an Ad*h*AQP1-transduced liver. No change in scattered light was observed when vesicles were mixed with isosmotic buffer (isosmolar). (**b**) Osmotic water permeability (P_f) calculated as described[27]. L, low P_f, calculated from the slow rate constant of a double-exponential fit. H, high P_f, calculated from the fast rate constant of a double-exponential fit. W, weighted P_f, calculated using the low and high P_f and their percentages of contribution to the total, that is, $W = (L \times 80 + H \times 20)/100$. Data are mean values ± s.e.m. from three independent vesicle preparations. *$P < 0.05$ as compared with canalicular vesicles from cholestatic liver treated with control vector.

Table 1. Liver serum parameters and body and liver weights in EE-cholestatic rats transduced with Ad*h*AQP1

	Non-cholestatic+saline	*Non-cholestatic controls+Adc*	*EE+saline*	*EE+Adc*	*EE+AdhAQP1*
ALP (U/L)	159 ± 29	182 ± 41	457 ± 81[a,b]	465 ± 39[a,b]	334 ± 37
AST (U/L)	144 ± 5	131 ± 21	127 ± 20	102 ± 1	139 ± 11
ALT (U/L)	25 ± 4	14 ± 3	25 ± 2	19 ± 2	22 ± 3
LDH (U/L)	987 ± 171	913 ± 13	811 ± 222	781 ± 132	637 ± 157
Body weight (g)	335 ± 9	368 ± 14	347 ± 9	333 ± 7	336 ± 7
Liver weight (g)	12.5 ± 0.3	12.9 ± 0.5	15.8 ± 0.4[a,b]	15.6 ± 0.4[a,b]	15.1 ± 0.3[a,b]

Abbreviations: Adc, control vector; EE, ethinylestradiol. EE-treated and non-cholestatic control rats were intrabiliary infused with Ad*h*AQP1, Adc or saline, as detailed in Materials and Methods. The experiments were performed 72 h after adenoviral infusion (that is, on day 6 after starting EE treatment). Data are means ± s.e.m. ($N = 3$–6). [a]$P < 0.05$ as compared with non-cholestatic controls. [b]$P < 0.05$ as compared with non-cholestatic+saline.

also studied the bile flow under stimulation. To stimulate hepatocyte (canalicular) bile flow, we made use of the physiological bile salt taurocholate, which is efficiently taken up by hepatocytes and excreted into bile.[20] Bile flow stimulated by taurocholate was 70% higher in cholestatic rats transduced with Ad*h*AQP1 than with control vector (Figure 3b). Taurocholate-induced bile flow (that is, taurocholate-stimulated bile flow over basal values) was increased threefold between these groups of rats (Figure 3b).

Thus, hepatic *h*AQP1expression in EE cholestatic rats significantly increased basal and bile salt-stimulated bile flow.

Thus, the AQP1-induced increase in canalicular water permeability of EE cholestatic rats significantly augmented basal and bile salt-stimulated bile flow.

Choleretic efficiency of bile salts in Ad*h*AQP1-transduced cholestatic rats

As bile formation by hepatocytes is an osmotic process primarily driven by bile salts, the increased canalicular water permeability observed in our studies (Figure 2) could have led to an increased water secretion in response to the output of bile salts. Thus, we studied whether the improved bile flow may be associated with an enhanced osmotic efficiency of excreted bile salts. The choleretic efficiency of endogenous bile salts (that is, volume of bile per µmol of excreted bile salt) was estimated from the slope of the relationship between bile flow and bile salt output during depletion of the bile salt pool by interruption of the enterohepatic circulation[21] (Figure 4a, left panel).

Cholestatic rats transduced with Ad*h*AQP1 showed a choleretic efficiency of total endogenous bile salts 45% higher than cholestatic rats transduced with control vector (Figure 4a, right panel). As individual endogenous bile salts may have different choleretic efficiencies, we assessed biliary bile salt composition by high-performance liquid chromatography. These studies indicated that the individual biliary bile salt composition was not significantly different between the above-mentioned groups of cholestatic rats (Figure 4b). Thus the enhanced choleretic efficiency of bile salts seems to be the result of the increased canalicular water permeability. This is supported by the estimated choleretic efficiency of taurocholate (µl of bile per µmol of excreted bile salt), estimated from the data in Figure 3: 5.1 ± 0.4 (non-cholestatic controls); 2.5 ± 1.0* (EE+Adc) and 5.9 ± 0.9 (EE+Ad*h*AQP1), *$P < 0.05$.

Our data suggest that the increased canalicular water permeability induced by *h*AQP1 transgene expression allowed a more efficient coupling between bile salts and water transport during bile secretion in cholestatic hepatocytes. As a result, there was an increased amount of bile-water osmotically driven by excreted bile salts. Bile consists mostly of water, and normal bile-water flow is necessary to keep small bile ducts open and to prevent the precipitation of biliary constituents so that flow is not

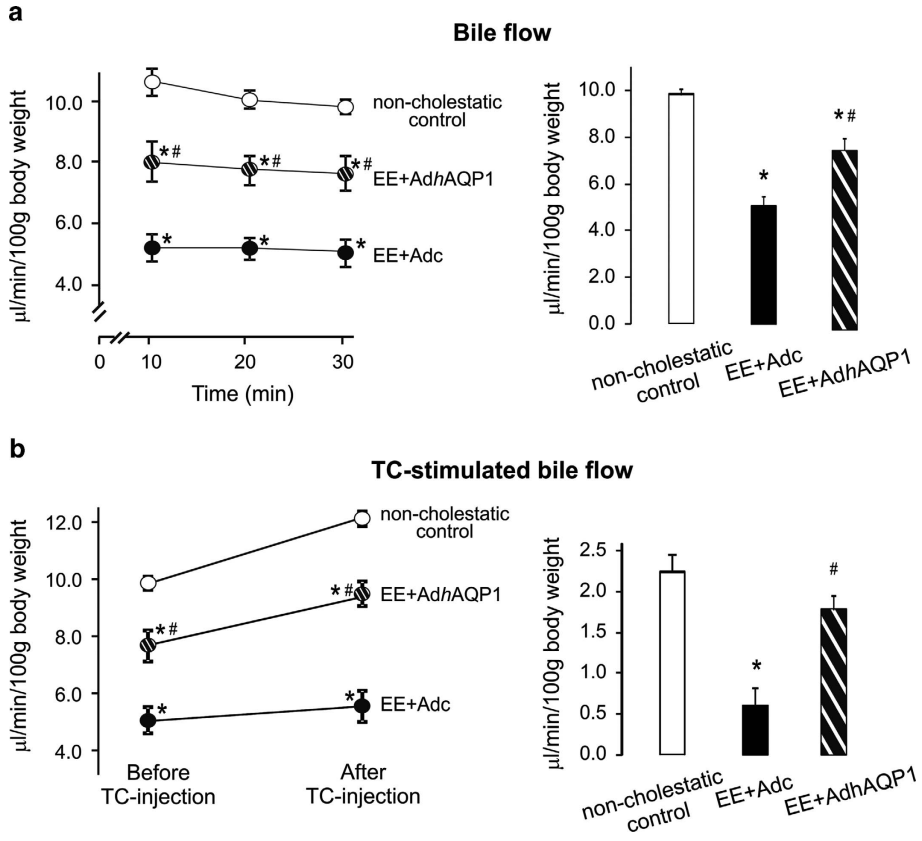

Figure 3. Bile flow in EE-cholestatic rats transduced with Ad*h*AQP1. The induction of cholestasis by EE and the delivery of vectors were detailed in Materials and Methods. The experiments were performed 72 h after adenoviral infusion (i.e., on day 6 after starting EE treatment). (**a**) Basal bile flow from cholestatic rats transduced with Ad*h*AQP1 or control vector. Values from normal rats transduced with control vector were included for the sake of comparison. Time course of basal bile flow (left panel) and average bile flow in 30-min bile collection period (right panel). (**b**) Taurocholate (TC)-stimulated bile flow from cholestatic rats transduced with Ad*h*AQP1 or control vector (left panel). TC-induced bile flow, that is, the TC-stimulated bile flow over basal values (right panel). Values from non-cholestatic rats transduced with control vector were included for the sake of comparison. Values from six animals per group are expressed as mean ± s.e.m. $^{*}P < 0.05$ versus non-cholestatic controls and $^{\#}P < 0.05$ versus EE.

obstructed.[22] Besides, biliary aqueous phase functions as the liquid vehicle for vesicles and micelles in bile to transport them to the intestine and thus permit their excretion. The function of biliary water is mostly self-protection[22] and therefore, a normal canalicular water transport would reduce the risk of bile secretory dysfunction.

We previously reported an AQP-mediated decrease of hepatocyte canalicular water permeability in other experimental model of cholestasis, that is, sepsis-associated cholestasis.[23] Thus, an Ad*h*AQP1-mediated improvement of bile secretion in sepsis-associated cholestasis may be anticipated. In fact, Ad*h*AQP1 administration may be beneficial to treat or prevent different liver diseases in which hepatocellular (non-obstructive) cholestasis occurs. In addition, Ad*h*AQP1-induced biliary water content may help to reduce bile viscosity in certain pathological states.[24]

Ursodeoxycholic acid is currently the only established drug for the treatment of cholestatic liver diseases.[25] As *hAQP1* gene transfer improved bile flow (Figure 3) and the retrograde biliary infusion is an approach that would be clinically feasible by means of endoscopic retrograde cholangiography, Ad*h*AQP1 delivery might be effective for treatment of bile secretory failure.

In conclusion, our data suggest that the adenoviral transfer of *hAQP1* gene to the livers of EE cholestatic rats improves bile flow by enhancing the AQP-mediated bile salt-induced canalicular water secretion. This novel finding might have potential therapeutic implications for cholestatic diseases.

MATERIALS AND METHODS

Animals and treatments

Adult male Wistar rats were maintained on a standard laboratory diet and water *ad libitum* and housed in a temperature- and humidity-controlled environment under a constant 12-h light–dark cycle. All animals received humane care, according to the Guide for the Care and Use of Laboratory Animals (National Institutes of Health). Protocols were approved by the local animal welfare committee. EE (Sigma-Aldrich, St Louis, MO, USA) (5 mg per kg body weight) was administered subcutaneously for five consecutive days. Non-cholestatic control rats received only the EE vehicle (propylene glycol). Under these conditions,[6] EE induced cholestasis as indicated by 50% bile flow reduction and cholestatic parameters (Table 1).

Adenoviral vectors

Ad*h*AQP1 is a replication-deficient serotype 5 recombinant adenovirus encoding *h*AQP1 and including a cytomegalovirus promoter and simian virus 40 polyadenylylation site. Ad*h*AQP1 was kindly donated by Dr Bruce Baum (NIDCR, NIH, Bethesda, MD, USA); details of the construction procedures have been described elsewhere.[7] The adenoviral vector used as control (Adc) is also a replication-deficient serotype 5 recombinant adenovirus that encodes β-galactosidase. Both vectors employed (Adc and Ad*h*AQP1) are first-generation constructs lacking the E1 region.

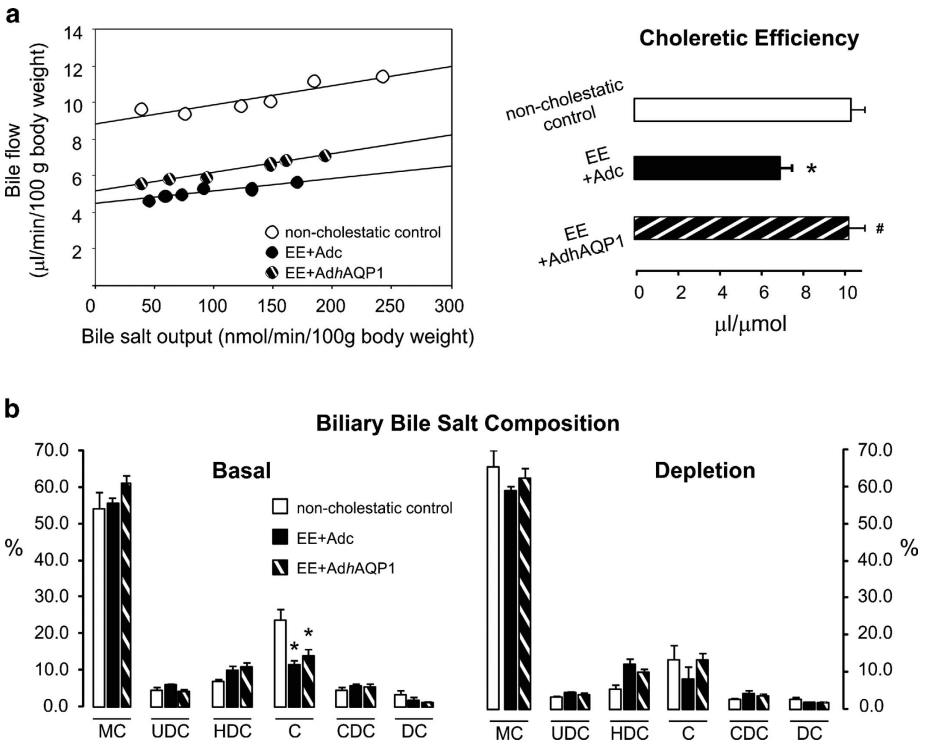

Figure 4. Choleretic efficiency of endogenous bile salts in EE-cholestatic rats transduced with Ad*h*AQP1. (**a**) Left Panel, representative relationships between bile flow and bile salt output in EE-cholestatic rats transduced with Ad*h*AQP1 (EE+Ad*h*AQP1) or control vector (EE+Adc) and non-cholestatic control rats. Bile was collected for 6 h in 1-h intervals. Interruption of the enterohepatic circulation of bile salts caused a progressive reduction of the biliary bile salt output. Individual time points for a representative animal per group are shown. Right Panel, choleretic efficiency of excreted bile salts was estimated from the slopes of the linear relationships between bile flow and bile salt output. Values from three animals per group are expressed as mean ± s.e.m. $^{*}P < 0.05$ from non-cholestatic control and $^{\#}P < 0.05$ from EE. (**b**) Individual biliary bile salt composition was determined in the 0–1-h (basal output) and 5–6-h (reduced output) samples after the enterohepatic interruption of bile salt circulation. Data are given as means ± s.e.m., C, cholate; CDC, chenodeoxycholate; DC, deoxycholate; HDC, hyodeoxycholate; MC, muricholate; $N = 3$ per group; $^{*}P < 0.05$ versus non-cholestatic control UDC, ursodeoxycholate.

In vivo delivery of recombinant adenovirus to the biliary tract

After the third EE injection, rats were anesthetized with a dose of ketamine (100 mg per kg body weight)/xylazine (15 mg per kg body weight, intraperitoneal). A 2-cm transversal laparotomy was made just below the xiphoid appendix to expose the duodenum. The duodenal antimesenteric wall was punctured with a 25G needle and a PE-10 polyethylene catheter (Intramedic, Clay Adams, Parsippany, NJ, USA) was introduced first into the lumen of the duodenum and then through the papilla of Vater 1 cm into the bile duct. A virus dose of 3×10^{10} pfu per liver suspended in 300 µl of sterile saline was retrogradely infused into the biliary tract during a period of 3 min. In additional control experiments, animals received only 300 µl of sterile saline. The catheter was maintained in place for 15 min to prevent backflow. After the procedure was completed the catheter was gently removed, the duodenal puncture and abdominal wall were sutured and the animal was allowed to recover. The experiments were performed 72 h after adenoviral infusion (that is, on day 6 after starting EE treatment). We performed, in advance, initial experiments to determine the optimal administration dose of adenovirus.

Bile secretion studies

After treatments, rats were anesthetized as mentioned above and maintained under this condition during bile collection. For this purpose, a middle abdominal incision was made and the common bile duct was cannulated with a PE-10 polyethylene tubing. Bile was collected for three 10-min periods. Thereafter, we injected bile salt taurocholate (Sigma, St Louis, MO, USA) (8 µmol per 100 g body weight, intravenous) to stimulate hepatocyte (canalicular) bile flow, and bile was collected for an additional 10-min period. Bile flow was determined by gravimetry, assuming a density of the bile of 1.0 g ml^{-1}.[6] At the end of bile collection, blood samples were taken by cardiac puncture, animals were euthanized by exsanguination and the livers harvested for evaluation.

Liver serum parameters

Activity of enzymes aspartate transaminase (AST), alanine transaminase (ALT), alkaline phosphatase (ALP) and lactate dehydrogenase (LDH) were determined in serum using commercial kits (Wiener Lab, Rosario, Argentina), according to the manufacturer's instructions.

Choleretic efficiency of endogenous bile salts

Rats were anesthetized and the bile duct was cannulated with a PE-10 polyethylene tubing. Bile was collected for 6 h in 1-h intervals. Bile flow was determined as mentioned above and total bile salt concentration was assessed using the 3α-hydroxysteroid dehydrogenase procedure.[26] The choleretic efficiency of endogenous bile salts (that is, volume of bile per µmol of excreted bile salt) was estimated from the slope of the relationship between bile flow and bile salt output.[21]

Biliary bile salt composition

In the first and sixth 1-h periods of bile collected for assessment of the choleretic efficiency of endogenous bile salts (see above),

individual bile salts were identified and quantified by high-performance liquid chromatography (Waters, Milford, MA, USA) by comparison with standard compounds, as reported.[27]

Hepatic plasma membrane fractions

Livers were homogenized by 15 up-down strokes with a loose-fitting Dounce homogenizer in four volumes of 0.3 M sucrose, containing 0.1 mM phenylmethylsulfonyl fluoride (Sigma) and 0.1 mM leupeptin (Chemicon, Millipore, Darmstadt, Germany). Liver homogenates were subjected to low-speed centrifugation to obtain postnuclear supernatants. Fractions enriched in plasma membranes were prepared from liver homogenates by centrifugation at 200 000 *g* for 60 min on a discontinuous 1.3 M sucrose gradient as previously described.[28] The plasma membrane band was removed, diluted to 0.3 M, and centrifuged at 200 000 *g* for 60 min to yield the plasma membrane fraction, which was further purified by centrifugation at 100 000 *g* for 90 min on a continuous (9–60%) sucrose gradient.[28] Purified plasma membranes were layered onto a discontinuous sucrose gradient composed of 31, 34 and 38% sucrose. After centrifugation at 270 000 *g* for 3 h, the band at the top of the 31% layer (canalicular plasma membrane) and the band at the top of the 38% layer (basolateral plasma membrane) were collected, diluted with washing buffer and spun at 200 000 *g* for 1 h.[29] Membrane proteins were determined according to the method of Lowry *et al.*[30] by using bovine serum albumin as standard.

Canalicular water permeability

The time course of canalicular vesicular volume was followed from changes in scattered light intensity at 450 nm by using a SX.18MVR stopped-flow spectrometer (Applied Photophysics, Surrey, UK) as previously described by our laboratory.[6] The osmotic water permeability coefficient (P_f) was calculated as described[6,29] using the equation: $P_f = K_{exp} V_o / A_v V_w \Delta C$, where K_{exp} is the fitted exponential rate constant, V_o is the initial mean vesicle volume, A_v is the mean vesicle surface, V_w is the molar volume of water and ΔC is the osmotic gradient. V_o and A_v were calculated by using a mean canalicular vesicle diameter of 160 ± 9 nm, assessed by morphometric analysis of electron micrographs.[6]

Immunoblotting

Western blotting of membrane fractions was performed as previously described by our laboratory[6,28] using rabbit affinity-purified AQP1 antibodies (1 μg ml^{-1}; Alpha Diagnostics International, San Antonio, TX, USA) and mouse β-actin antibodies (1 μg ml^{-1}; Sigma) and horseradish peroxidase-conjugated corresponding secondary antibodies (DakoCytomation, Glostrup, Denmark). Protein bands were detected by enhanced chemiluminescence detection system (ECL, Amersham Pharmacia Biotech, Thermo Scientific, Rockford, NJ, USA). Autoradiographs were obtained by exposing the membranes to Kodak XAR films (Eastman Kodak, Rochester, NY, USA). Densitometric analysis of the developed bands was performed using ImageJ software (U.S. National Institutes of Health, Bethesda, MD, USA).[31]

Immunohistochemistry

Livers were perfused with phosphate-buffered saline to eliminate the blood and then they were fixed, processed and embedded in paraffin as described.[6,28] AQP1 was localized with affinity-purified antibodies (10 μg ml^{-1}; Alpha Diagnostics International) and horseradish peroxidase-conjugated secondary antibodies (DakoCytomation) on serial 5-μm sections. Controls were performed by omitting the primary antibodies. Images were captured with an E 600 photomicroscope equipped with a DMX 1200 digital camera (Nikon, Kawasaki, Japan). The slides were developed by incubating with 0.06% 3,3-diaminobenzidine and 0.01% H_2O_2 for 5 min and counterstained using hematoxylin.

Confocal immunofluorescence microscopy and image analysis

Fixed liver sections were permeabilized and blocked with 0.2% Triton X-100/bovine serum albumin 3% for 10 min and incubated overnight at 4 °C with rabbit affinity-purified AQP1 antibodies (10 μg ml^{-1}). After washing, samples were incubated with Alexa 488-conjugated goat anti-rabbit secondary antibody (Molecular Probes, Eugene, OR, USA) for 1 h. Samples were washed, incubated with 4′,6-diamidino-2-phenylindole (Molecular Probes) (50 μM) for 10 min and mounted with ProLong (Molecular Probes). Fluorescence localization was detected by confocal microscopy (Nikon C1PlusSiR with inverted microscope Nikon TE2000, Melville, NY, USA). Images were collected with the same confocal settings in each set of experiments. With these settings no autofluorescence was detected. Controls omitting primary or secondary antibodies revealed no labeling. For the sake of clarity, contrast and brightness adjustments were equally applied to the entire images via Adobe Photoshop software (San Jose, CA, USA).

Transduction efficiency of Ad*h*AQP1 in hepatocytes from cholestatic rats was estimated from the confocal immunofluorescence images using the NIH ImageJ program.[31] Several images with around 400 cells each were used. Images corresponding to the Adc vector were used as fluorescence background for setting the scale for image analysis. Positively stained hepatocytes represent roughly 20% of total cells counted.

Statistical analysis

Data are expressed as means ± s.e.m. Significance was determined by Student's *t*-test or the one-way analysis of variance, Tukey's test. $P < 0.05$ was considered statistically significant.

CONFLICT OF INTEREST

The authors declare no conflict of interest.

ACKNOWLEDGEMENTS

We thank R Rassia for helping us in stopped-flow studies, J Monti for surgical assistance and A Martínez for immunohistochemistry assays. This work was supported by Grant PIP 0244 from Consejo Nacional de Investigaciones Científicas y Técnicas (CONICET) to RAM.

REFERENCES

1 Lee J, Boyer JL. Molecular alterations in hepatocyte transport mechanisms in acquired cholestatic liver disorders. *Semin Liver Dis* 2000; **20**: 373–384.
2 Crocenzi FA, Sánchez Pozzi EJ, Pellegrino JM, Favre CO, Rodríguez Garay EA, Mottino AD *et al.* Beneficial effects of silymarin on estrogen-induced cholestasis in the rat: a study in vivo and in isolated hepatocyte couplets. *Hepatology* 2001; **34**: 329–339.
3 King LS, Kozono D, Agre P. From structure to disease: the evolving tale of aquaporin biology. *Nat Rev Mol Cell Biol* 2004; **5**: 687–698.
4 Marinelli RA, Lehmann GL, Soria LR, Marchissio MJ. Hepatocyte aquaporins in bile formation and cholestasis. *Front Biosci (Landmark Ed)* 2011; **16**: 2642–2652.
5 Portincasa P, Calamita G. Water channel proteins in bile formation and flow in health and disease: when immiscible becomes miscible. *Mol Aspects Med* 2012; **33**: 651–664.
6 Carreras FI, Lehmann GL, Ferri D, Tioni MF, Calamita G, Marinelli RA. Defective hepatocyte aquaporin-8 expression and reduced canalicular membrane water permeability in estrogen-induced cholestasis. *Am J Physiol Gastrointest Liver Physiol* 2007; **292**: G905–G912.
7 Delporte C, O'Connell BC, He X, Lancaster HE, O'Connell AC, Agre P *et al.* Increased fluid secretion after adenoviral-mediated transfer of the aquaporin-1 cDNA to irradiated rat salivary glands. *Proc Natl Acad Sci USA* 1997; **94**: 3268–3273.

8 Shan Z, Li J, Zheng C, Liu X, Fan Z, Zhang C *et al.* Increased fluid secretion after adenoviral-mediated transfer of the human aquaporin-1 cDNA to irradiated miniature pig parotid glands. *Mol Ther* 2005; **11**: 444–451.
9 Baum BJ, Alevizos I, Zheng C, Cotrim AP, Liu S, McCullagh L *et al.* Early responses to adenoviral-mediated transfer of the aquaporin-1 cDNA for radiation-induced salivary hypofunction. *Proc Natl Acad Sci USA* 2012; **109**: 19403–19407.
10 Marinelli RA, Tietz PS, Pham LD, Rueckert L, Agre P, LaRusso NF. Secretin induces the apical insertion of aquaporin-1 water channels in rat cholangiocytes. *Am J Physiol* 1999; **276**: G280–G286.
11 Terao R, Honda K, Hatano E, Uehara T, Yamamoto M, Yamaoka Y. Suppression of proliferative cholangitis in a rat model with direct adenovirus-mediated retinoblastoma gene transfer to the biliary tract. *Hepatology* 1998; **28**: 605–612.
12 Kuriyama S, Yoshiji H, Nakai S, Deguchi A, Uchida N, Kimura Y *et al.* Adenovirus-mediated gene transfer into rat livers: comparative study of retrograde intrabiliary and antegrade intraportal administration. *Oncol Rep* 2005; **13**: 69–74.
13 Monte MJ, Badia MD, Palomero F, el-Mir MY, Alonso JR, Marin JJ. Effects of selective zonal injury on bile acid-induced bile flow in the isolated rat liver. *Am J Physiol* 1993; **264**: G1103–G1111.
14 Zheng C, Goldsmith CM, Mineshiba F, Chiorini JA, Kerr A, Wenk ML *et al.* Toxicity and biodistribution of a first-generation recombinant adenoviral vector, encoding aquaporin-1, after retroductal delivery to a single rat submandibular gland. *Hum Gene Ther* 2006; **17**: 1122–1133.
15 Jiang X, Ren Y, Williford JM, Li Z, Mao HQ. Liver-targeted gene delivery through retrograde intrabiliary infusion. In: Manfred O, David O (eds) *Nanotechnology for Nucleic Acid Delivery: Methods and Protocols, Methods Mol Biol*. Humana Press: New Jersey, 2013, pp 275–284.
16 Tominaga K, Kuriyama S, Yoshiji H, Deguchi A, Kita Y, Funakoshi F *et al.* Repeated adenoviral administration into the biliary tract can induce repeated expression of the original gene construct in rat livers without immunosuppressive strategies. *Gut* 2004; **53**: 1167–117.
17 Jessner W, Zsembery A, Graf J. Transcellular water transport in hepatobiliary secretion and role of aquaporins in liver. *Wien Med Wochenschr* 2008; **158**: 565–569.
18 Arrese M, Macias RI, Briz O, Perez MJ, Marin JJ. Molecular pathogenesis of intrahepatic cholestasis of pregnancy. *Expert Rev Mol Med* 2008; **10**: e9.
19 Pauli-Magnus C, Meier PJ, Stieger B. Genetic determinants of drug-induced cholestasis and intrahepatic cholestasis of pregnancy. *Semin Liver Dis* 2010; **30**: 147–159.
20 Hung DY, Siebert GA, Chang P, Roberts MS. Hepatic pharmacokinetics of taurocholate in the normal and cholestatic rat liver. *Br J Pharmacol* 2005; **145**: 57–65.
21 Koopen NR, Wolters H, Havinga R, Vonk RJ, Jansen PL, Müller M *et al.* Impaired activity of the bile canalicular organic anion transporter (Mrp2/cmoat) is not the main cause of ethinylestradiol-induced cholestasis in the rat. *Hepatology* 1998; **27**: 537–545.
22 Hofmann AF. Overview of Bile Secretion. In: Pollock DM (ed) *Comprehensive Physiology*. John Wiley & Sons: Hoboken NJ, 2011, pp 549–566.
23 Lehmann GL, Carreras FI, Soria LR, Gradilone SA, Marinelli RA. LPS induces the TNF-alpha-mediated downregulation of rat liver aquaporin-8: role in sepsis-associated cholestasis. *Am J Physiol Gastrointest Liver Physiol* 2008; **294**: G567–G575.
24 Reinhart WH, Näf G, Werth B. Viscosity of human bile sampled from the common bile duct. *Clin Hemorheol Microcirc* 2010; **44**: 177–182.
25 Roma MG, Toledo FD, Boaglio AC, Basiglio CL, Crocenzi FA, Sánchez Pozzi EJ. Ursodeoxycholic acid in cholestasis: linking action mechanisms to therapeutic applications. *Clin Sci (Lond)* 2011; **121**: 523–544.
26 Jarabak J, Talalay P. Stereospecificity of hydrogen transfer by pyridine nucleotide-linked hydroxysteroid dehydrogenases. *J Biol Chem* 1960; **235**: 2147–2151.
27 Tietz PS, Thistle JL, Miller LJ, LaRusso NF. Development and validation of a method for measuring the glycine and taurine conjugates of bile acids in bile by high-performance liquid chromatography. *J Chromatogr* 1984; **336**: 249–257.
28 Carreras FI, Gradilone SA, Mazzone A, García F, Huang BQ, Ochoa JE *et al.* Rat hepatocyte aquaporin-8 water channels are down-regulated in extrahepatic cholestasis. *Hepatology* 2003; **37**: 1026–1033.
29 Marinelli RA, Tietz PS, Caride AJ, Huang BQ, LaRusso NF. Water transporting properties of hepatocyte basolateral and canalicular plasma membrane domains. *J Biol Chem* 2003; **278**: 43157–43162.
30 Lowry OH, Rosebrough NJ, Farr AL, Randal RJJ. Protein measurement with the Folin phenol reagent. *J Biol Chem* 1951; **193**: 265–275.
31 Rasband, WS. US National Institutes of Health, Bethesda, MD, USA, 1997–2011 http://imagej.nih.gov/ij/.